

## New method of synthesizing $\text{In}_2\text{O}_3$ nanoparticles for application in volatile organic compounds (VOCs) gas sensors

B. L. ZHU \*

Department of Physics, Wuhan University, Hubei, Wuhan 430072, People's Republic of China  
E-mail: zhubailin97@hotmail.com

C. S. XIE, D. W. ZENG, A. H. WANG, W. L. SONG

Department of Materials Science and Engineering, Huazhong University of Science and Technology, Hubei, Wuhan 430074, People's Republic of China

X. Z. ZHAO

Department of Physics, Wuhan University, Hubei, Wuhan 430072, People's Republic of China

Published online: 16 September 2005

$\text{In}_2\text{O}_3$  nanoparticles have increasingly attracted interest over the past decade due to their novel properties [1]. They are usually synthesized by using chemical routes such as sol-gel and solid-state reaction methods [2, 3]. However, there are some limitations such as a low yield rate, impurity pollution and agglomerates in these techniques. Recently, we have developed a new specific device in which inductive resource and continuous wave  $\text{CO}_2$  laser beam were compounded to synthesize metal and their oxide nanoparticles, which can overcome the above-mentioned limitations [4]. Using this hybrid induction and laser heating (HILH) method, refractory cobalt amorphous or crystalline nanoparticles as well as  $\text{Sb}_2\text{O}_3$  nanoparticles were synthesized [5, 6]. Also tetrapod-like  $\text{ZnO}$  nanowiskers were synthesized using this novel method and its yield rate can reach several kilograms per hour [7]. In this study, the  $\text{In}_2\text{O}_3$  nanoparticles were synthesized by means of HILH, and the characteristics of the nanoparticles was systematically investigated by transmission electron microscope (TEM) and X-ray diffraction (XRD).

As a gas sensing material,  $\text{In}_2\text{O}_3$  has been extensively applied to detect  $\text{O}_3$ ,  $\text{NO}_2$  and  $\text{CO}$  etc. [8–10]. We believe that the gas-sensing properties of  $\text{In}_2\text{O}_3$  for volatile organic compounds (VOCs), especially toxic VOCs that are harmful to human health and the environment, have not been broadly studied. So the gas-sensing properties for five VOCs (benzene, toluene, xylene, acetone and alcohol) of thick films based on as-synthesized  $\text{In}_2\text{O}_3$  nanoparticles were studied in this letter.

The experimental setup of HILH is described in the literature elsewhere [6]. The experimental procedures were as follows: the metallic indium was heated to a certain temperature by induction-heating in a vacuum chamber with a flowing mixed  $\text{Ar} + \text{O}_2$  gas at a pressure of  $1.0 \times 10^4$  Pa, where the oxygen partial pressure was kept fixed at about  $2 \times 10^3$  Pa by controlling the oxygen flux. Subsequently, the continuous wave  $\text{CO}_2$

laser beam was focused at the liquid surface. The focused beam diameter was 4 mm and the laser power was 1600 W, which gave a power density in the order of  $10^4$   $\text{W}/\text{cm}^2$ . Finally the nanoparticles were obtained from the collection chamber for further examination. A JEM-2000 transmission electron microscope (TEM) was employed to observe the morphology of as-synthesized nanoparticles. Its phase structure was identified by X-ray diffraction (XRD) with  $\text{Cu K}\alpha 1$  incident radiation. The preparation of thick films based on nanoparticles, and the measurement of resistance and gas-sensing properties for the thick film are described in detail in the literature [4]. The gas sensitivity,  $S$ , is defined as the ratio ( $R_a/R_g$ ) of resistance in air ( $R_a$ ) to that in detecting gas ( $R_g$ ).

Fig. 1 presents the typical morphology of  $\text{In}_2\text{O}_3$  nanoparticles prepared by the HILH method, indicating that the powders consist of small quadrate-like nanoparticles with size ranging from about 20–50 nm. The XRD pattern of the nanoparticles reveals that as-synthesized powder consists of a single  $\text{In}_2\text{O}_3$  phase, as shown in Fig. 2. Chen *et al.* [11] reported that quasi-spherical  $\text{In}_2\text{O}_3$  nanoparticles with maximal size of approx. 30 nm were produced by the atomizing-combustion technique, and the color of the powders was buff. Quan *et al.* [2] reported that the mean size of  $\text{In}_2\text{O}_3$  powders prepared by the sol-gel method was about 50–60 nm. In literature [3],  $\text{In}_2\text{O}_3$  powders with a mean grain size of about 25 nm were prepared by the solid-state reaction method.

Fig. 3 shows the resistance of  $\text{In}_2\text{O}_3$  thick film as a function of working temperature. From Fig. 3, we can observe that the resistance of the thick films is about  $10^5$   $\Omega$  at room temperature, then it begins to drop steeply until the temperature exceeds  $150^\circ\text{C}$ . It is worth noting that the resistance of  $\text{In}_2\text{O}_3$  thick films increases slowly in range of  $150$ – $270^\circ\text{C}$ , then drops slowly over the range of  $270$ – $420^\circ\text{C}$ . When the temperature is higher than  $420^\circ\text{C}$ , the resistance drops steeply again.

\* Author to whom all correspondence should be addressed.

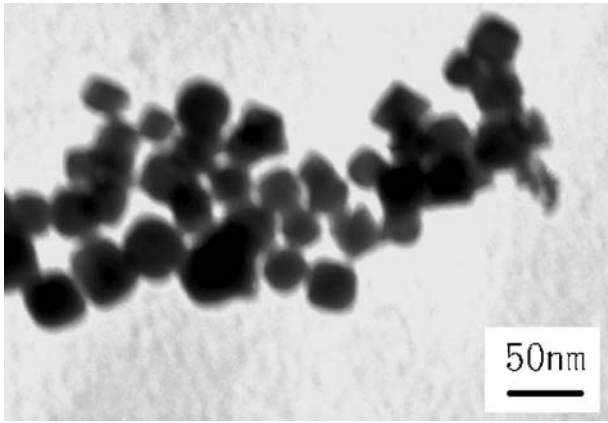


Figure 1 TEM image of  $\text{In}_2\text{O}_3$  nanoparticles produced by HILH.

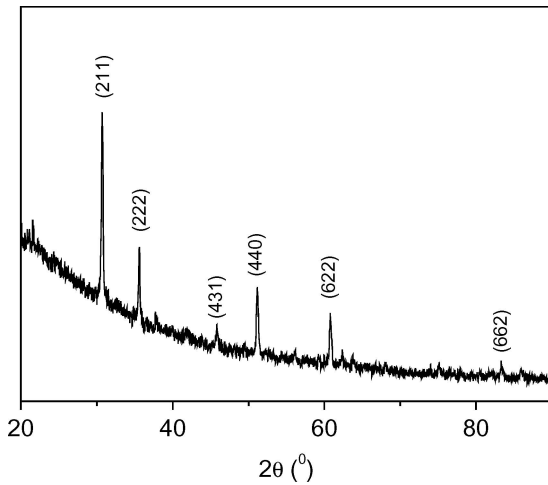


Figure 2 XRD pattern of obtained  $\text{In}_2\text{O}_3$  nanoparticles.

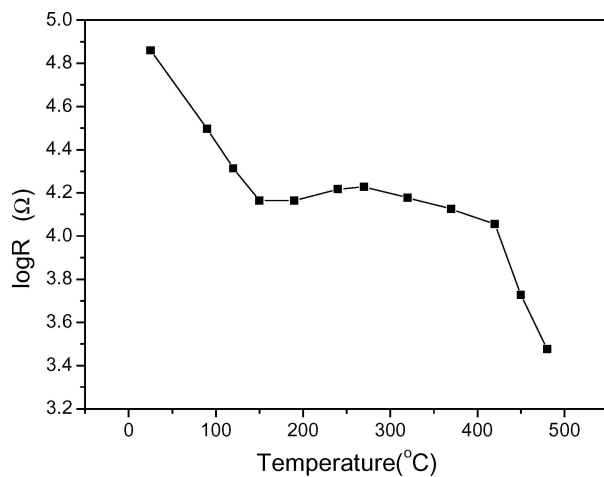


Figure 3 Temperature dependence of the resistance in air of  $\text{In}_2\text{O}_3$  thick film.

It is obvious that the resistance change largely depends on the operating temperature, which is attributed to the change of intrinsic conductance and surface adsorbed oxygen with temperature.

In the case of  $\text{In}_2\text{O}_3$  thick films, the electrons are extracted from the oxygen vacancies and the interstitial indium atoms [2]. The defect reactions are described

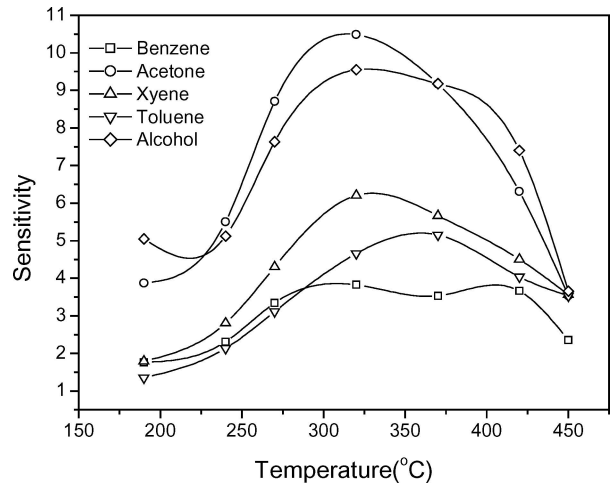
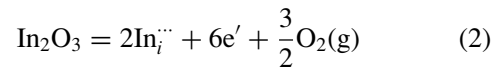
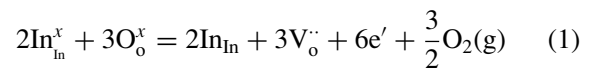


Figure 4 The sensitivity versus operating temperature of  $\text{In}_2\text{O}_3$  thick film.

as follows:



With increasing temperature, the intrinsic conductance increases monotonously, but the grain surface of the thick film can adsorb much oxygen and the surface adsorbed oxygen captures electrons to produce  $\text{O}_2^-$ ,  $\text{O}_2^{2-}$  and  $\text{O}^-$ , which produce the resistance increase. So the resistance change of the films depends on the above-mentioned, two opposing factors. At lower temperature, the intrinsic conductance increase surpasses the conductance decrease caused by adsorbed oxygen, so the resistance continues dropping until  $T > 150^\circ\text{C}$ , where adsorbed oxygen or  $\text{O}^-$  acquires enough energy to transform into  $\text{O}^-$  or  $\text{O}_2^{2-}$ , causing the resistance to slowly increase from 150 to 270  $^\circ\text{C}$ , then slowly drop from 270  $^\circ\text{C}$  to 420  $^\circ\text{C}$ . When  $T > 420^\circ\text{C}$ , intrinsic conductance obviously dominates the situation again with the desorption of oxygen, making the curve fall steeply.

Fig. 4 illustrates the sensitivity to each of the five VOCs of acetone, benzene, alcohol, xylene and toluene tested as a function of temperature. Obviously, the sensitivity goes through a maximum at around 320  $^\circ\text{C}$  for all the organic vapors. The VOCs readily react with the oxygen ions and liberate electrons to the conduction band, accompanied by an increase in conductivity of the film, when they are in contact with the surface of the  $\text{In}_2\text{O}_3$  film (at the proper elevated temperature). So the decreasing level of resistance, i.e. sensitivity, is dependent on the change of chemisorbed oxygen ions on the surface. The process can be represented as follows:



The increase in sensitivity with operating temperature can be attributed to the fact that the amount of

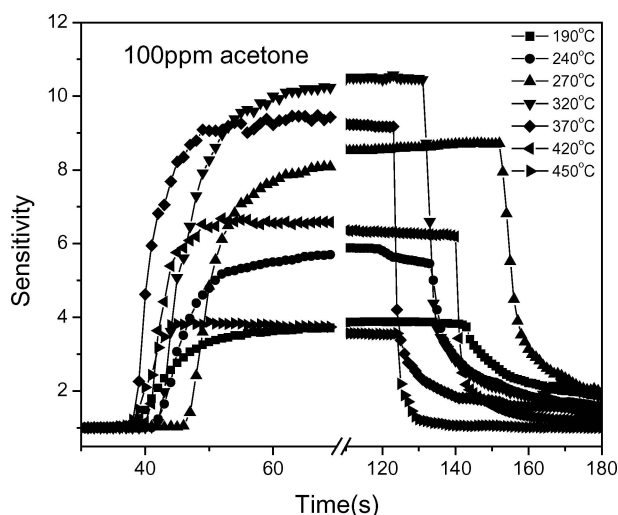


Figure 5 Sensitivity as a function of time of  $\text{In}_2\text{O}_3$  thick film at various temperatures.

chemisorbed oxygen ions gradually increases as discussed above and the thermal energy obtained is high enough to overcome the activation energy barrier to the reaction, while the reduction in sensitivity above  $320^\circ\text{C}$  is due to a gradual decrease in the amount of chemisorbed oxygen ions and/or the enhancement of desorption of oxygen.

The sensitivity is related to functional groups of organic vapor. Among the five organic vapors the films exhibit the highest sensitivity to acetone, next to alcohol. Of the three kinds of organic vapors with phenyl, xylene gives the highest sensitivity, followed by toluene, and the sensitivity to benzene is lowest, which coincides with the number of methyl groups involved.

Fig. 5 shows the typical change in sensitivity of the films as a function of time maintained at different operating temperatures, after injecting 100 ppm acetone into the chamber. The results show that the operating temperature influences not only the sensitivity, but also the response-recovery time of the thick films. It is observed that the response-recovery time is long at lower temperature, and it becomes short when the operating temperature is higher than or equal to  $320^\circ\text{C}$ . Generally speaking, the response-recovery time of the films

decreases with decreasing temperature because the VOCs adsorption, oxidation and desorption are all thermally activated reactions, which are sensitive to temperature. In addition, the response-recovery time of sensors also depends on the vapor species and its concentration.

In conclusion,  $\text{In}_2\text{O}_3$  nanopowders formed by (HILH) consist of small quadrate-like particles with sizes ranging from about 20–50 nm. The operating temperature influences the resistance, sensitivity and response-recovery time for VOCs of  $\text{In}_2\text{O}_3$  thick films. At  $320^\circ\text{C}$ , the highest sensitivity is obtained, and the response-recovery time is shortest.

### Acknowledgments

The financial support by the Key Project for Science and Technology Research of Ministry of Education (Grant No. 00084), Science and Technology Planning Project of Wuhan (Grant No. 20011007088–5) is gratefully acknowledged.

### References

1. B. L. YU, C. S. ZHU, F. X. GAN, *et al.*, *Opt. Mater.* **7** (1997) 103.
2. B. F. QUAN, Z. Y. ZHAO, T. ZHANG, *et al.*, *Instrum. Technol. Sensor* (2001) 12 (in chinese).
3. J. Q. XU, Y. L. LIU and X. S. NIU, *J. Inorg. Mater.* **17** (2002) 367 (in chinese).
4. B. L. ZHU, D. W. ZENG, C. S. XIE, *et al.*, *J. Mater. Sci.: Mater. Electron.* **14** (2003) 521.
5. C. S. XIE, J. H. HU, R. WU, *et al.*, *Nanostruct. Mater.* **11** (1999) 1061.
6. D. W. ZENG, B. L. ZHU and C. S. XIE, *et al.*, *Mater. Sci. Eng. A* **336** (2004) 332.
7. R. WU, C. S. XIE, H. XIA, *et al.*, *J. Cryst. Growth* **217** (2000) 274.
8. G. FAGLIA, B. ALLIERI, E. COMINI, *et al.*, *Sensors Actuat. B* **57** (1999) 188.
9. H. STEFFES, C. IMAWAN, F. SOLZBACHER, *et al.*, *ibid.* **68** (2000) 249.
10. T. V. BELYSHEVA, E. A. KAZACHKOV and E. E. GUTMAN, *J. Anal. Chem.* **56** (2001) 676.
11. S. Z. CHEN and Z. M. YIN, *Mater. Sci. Eng.* **16** (1998) 60 (in chinese).

Received 6 May 2004

and accepted 24 March 2005